Supporting Information

Porous Polyurea Supported Pd Catalyst: Easy Preparation, Full Characterization and High Activity and Reusability in Reduction of Hexavalent Chromium in Aqueous System

Muhammad Sohail Bashir, Xubao Jiang, Xingjie Yang, and Xiang Zheng Kong**

College of Chemistry and Chemical Engineering, University of Jinan, Jinan 250022, China

Correspondence authors:

E-mail addresses: chm_jiangxb@ujn.edu.cn (X. Jiang), xzkong@ujn.edu.cn (X. Z. Kong)

EXPERIMENTAL SECTION

Materials. Toluene diisocyanate (TDI, 80% of 2,4- and 20% of 2,6-isomers, industrial grade, from Beijing Keju Chemicals Ltd.); Dichloromethane (DCM, AP, from Tianjin Fuyu Chemical Co. Ltd.); Acetone (AP, from Tianjin Damao Chemicals); Sodium borohydride ($NaBH_4$, AP), Pd supported on activated carbon (Pd@C, 10 wt% of Pd) and deuterated dimethyl sulfoxide (DMSO-d_6, 99.9%) were purchased from Sigma-Aldrich. Palladium acetate ($Pd(OAc)_2$), potassium dichromate ($K_2Cr_2O_7$), potassium bromide (KBr), formic acid (FA), and sodium formate (SF), all AP grade, were purchased from Aladdin Biochemical Technology Co. Ltd. All the chemicals were used as received. Ultra-pure water from Millipore (Simplicity, USA) was used throughout this work.

Preparation of Pd@PPU. Pd@PPU was prepared in two consecutive steps. PPU was prepared first via precipitation polymerization of TDI with water in a binary solvent of water-acetone based on a reported process (Han, H. et al. *RSC Adv.* **2014**, *4*, 33520–33529). In brief, water (27 g) and acetone (63 g) were mixed in a round-bottom flask of 150 mL capacity at 30 °C. TDI (10 g) was added into the flask at a fixed rate (10 mL/h) under stirring at 300 rpm. After the completion of TDI addition, polymerization was continued for 2 h at 30 °C. At the end of polymerization, solid PPU was separated out by filtration, rinsed with acetone, and dried under vacuum at 60 °C for 5 h. The solvent was easily separated upon the stirring stopped, and can be reused for unlimited times. In the second step, $Pd(OAc)_2$ was

immobilized onto PPU. To this end, $Pd(OAc)_2$ (0.15 g) was dissolved in DCM (100 mL) in a round bottom flask of 250 mL capacity, equipped with a stirrer and condenser. PPU (1.00 g) was added into $Pd(OAc)_2$ solution in DCM under stirring (250 rpm) at room temperature to achieve the immobilization. To check the immobilization progress, samples were taken from the mixture of PPU and $Pd(OAc)_2$ solution, filtered to separate PPU out and diluted with DCM, followed by UV-vis absorbance test at 374 nm (Figure S1 here below) using a spectrophotometer (Lambda 35, Perkin-Elmer), to measure the remaining concentration of $Pd(OAc)_2$ in the supernatant. At the end of the process, PPU with $Pd(OAc)_2$ immobilized on their surface, $Pd(OAc)_2$@PPU, was separated out by filtration, rinsed with DCM for 5 times, and dried under vacuum at 60 °C. DCM was easily separated from the polymerization upon the stirring halted, and could be reused for unlimited times. The composite $Pd(OAc)_2$@PPU (0.50 g) was transferred into a freshly prepared aqueous solution of $NaBH_4$ (0.50 M, 20 mL) in a round bottom flask (50 mL capacity), and the whole was gently stirred at room temperature for 1 h in order to reduce $Pd(OAc)_2$ to Pd element to get Pd@PPU, a powder with dark green color after filtration, rinsed with water for 5 times, and dried under vacuum at 60 °C for 5 h.

Characterization of PPU, $Pd(OAc)_2$@PPU and Pd@PPU. Morphologies of PPU, $Pd(OAc)_2$@PPU, and Pd@PPU were observed under optical microscope (OM, BX-51, Olympus), scanning electronic microscope (SEM, Quanta FEG-250, FEI). Brunauer-Emmett-

Teller (BET, Nora 200E, Quantachrome) characterization was used to determine their specific surface area and porous properties. The presence of Pd in the samples was checked using energy-dispersive X-ray spectroscopy (EDS, X-Max50, Oxford), and immobilized Pd amount was determined using inductive coupled plasma optical emission spectrometer (ICP-OES, Optima 5300DV, Perkin-Elmer). $Pd(OAc)_2$@PPU and Pd@PPU were also subjected to high resolution transmission electron microscopy analysis (HRTEM, JEM-2100F, JEOL) to estimate the size and size distribution of Pd-NPs on their surface. X-ray photoelectron spectroscopy (XPS, ESCALAB 250Xi, Thermo Fisher Scientific) was used to detect atomic state of Pd in the composites $Pd(OAc)_2$@PPU and Pd@PPU. Selected samples were analysed by FTIR (Vertex 70, Brüker) by compressing the sample in KBr pellet, and by magnetic resonance spectroscopy to Carbon-13 nuclear (NMR, Advance III 400M, Brüker) using DMSO-d_6 as the solvent. Powder X-ray diffraction (XRD) was performed on a diffractometer (D8 Focus, Brüker). Chemisorptions were performed to determine Pd dispersion in the catalyst using AutoChem II 2920 (Micromeritics). UV absorbance was determined by a spectrophotometer of Lambda 35 (Perkin-Elmer), equipped with a cell holder, connected both ends to a water bath (Haake, K20) through silicone tubing, with water circulating from and to the water bath and passing through the cell holder. With this apparatus installation, the temperature was readily controlled in between 3 °C and 90 °C.

Catalytic Activity and Recycled Use of Pd@PPU in Cr(VI) Reduction. The composite Pd@PPU was used as a catalyst in the reduction of Cr(VI) to Cr(III) in water in the presence of FA and SF. For a typical run, an aqueous solution of $K_2Cr_2O_7$ (10.00 mL, 2.04 mM) was charged in a reaction bottle placed in a water bath at 25 °C, followed by addition of Pd@PPU of 6.0 mg (2.55 wt% of Pd). The reduction was started upon addition of FA (225 μL, 5.97 mmol) and SF (170.0 mg, 2.50 mmol) with the mixture under constant and gently stirring, making the reaction mixture with $K_2Cr_2O_7$ at 2.00 mM, FA at 0.583 M, SF at 0.244 M, and Pd@PPU at 0.59 mg/mL. During the reduction, samples were taken (200 μL each) from the reaction mixture, diluted to 2.00 mL and subjected to UV-vis absorbance at 350 nm to monitor the remaining Cr(VI) concentration (Huang, Y. et al. *ACS Appl. Mater. Interfaces* **2012**, *4*, 3054–3061). At end of the reduction, Pd@PPU was separated out and an excessive amount of NaOH was added to the supernatant to ascertain the formation of Cr(III). Upon NaOH addition, the supernatant turned green, indicating the formation of hexahydroxochromate (III) (Huang, Y. et al. *ACS Appl. Mater. Interfaces* **2012**, *4*, 3054–3061). After a full reduction of Cr(VI), Pd@PPU was recovered, washed with water, dried at 80 °C for 6 h under vacuum, and reused for subsequent Cr(VI) reduction under exactly the same conditions. Once a deactivation of the catalyst activity observed, the catalyst was regenerated by heating it in a tubular furnace (TCGC/1700, Tongcoo, Shanghai) at 180 °C for

2 h under N_2 atmosphere. After cooling down to room temperature, the regenerated catalyst was used for Cr(VI) reduction under exactly the same conditions.

To elucidate the cause of the slight deterioration of the catalyst in its recycled use, parallel tests of Cr(VI) reduction using catalyst pretreated by H_2, CO and CO_2, respectively, were also conducted, in which exactly the same procedure as for the virgin catalyst described above was used, except a 24 h contact with the gas used for catalyst pre-treatment prior to the addition of FA to start of the process. With H_2 as example, the catalyst was pretreated as following: catalyst Pd@PPU (6.0 mg, 2.55 wt% of Pd), $K_2Cr_2O_7$ aqueous solution (10.00 mL, 2.04 mM) and SF (170.0 mg, 2.50 mmol) was added consecutively into a pressure bottle of 300 mL capacity, vacuumized, and filled up with H_2. The bottle was then left shelf-standing for 24 h, and the reduction was started by injection of FA (225 μL, to make its concentration at 0.583 M). Cr(VI) reduction was monitored by UV-vis absorbance as above.

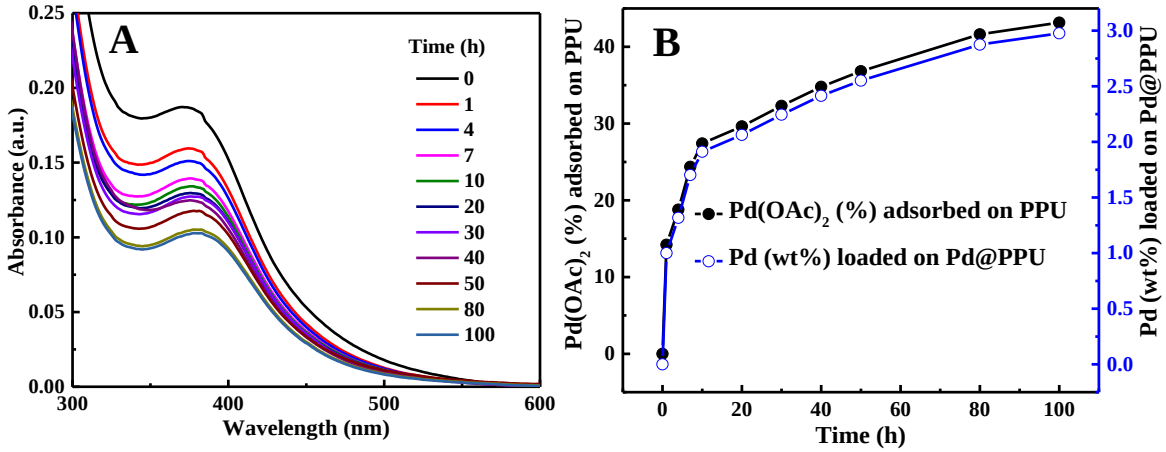

Figure S1. Changes in UV-vis absorbance spectra of $Pd(OAc)_2$ solution in DCM (A), $Pd(OAc)_2$ loading rate and corresponding Pd loaded on PPU (B) from $Pd(OAc)_2$ (0.15 g) solution in DCM (100 mL)

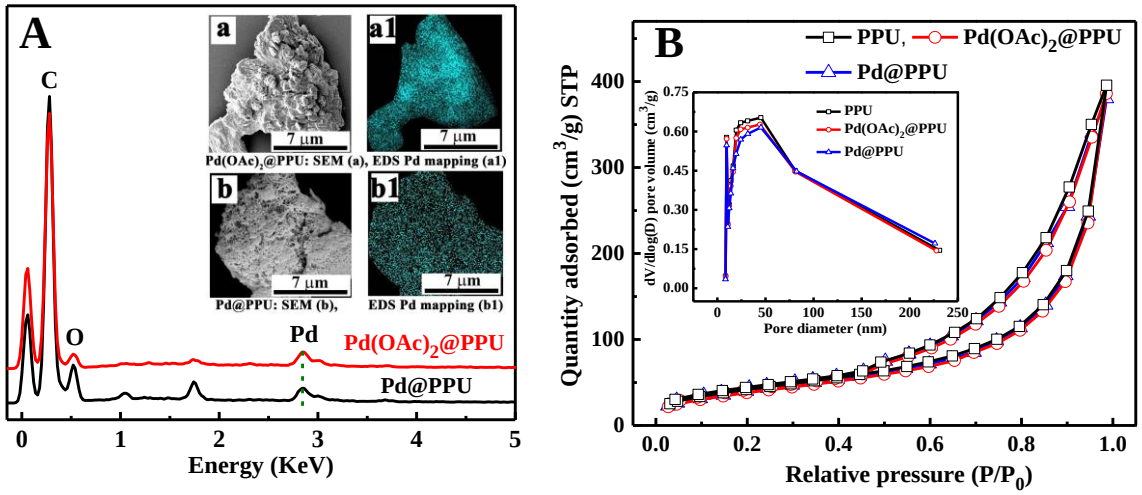

Figure S2. EDS spectrum and Pd mapping (inset) of $Pd(OAc)_2$@PPU and Pd@PPU (A), N_2 adsorption-desorption as function of relative pressure (P/P_0) by BET for PPU, $Pd(OAc)_2$@PPU and Pd@PPU (B) (inset B is their pore size distributions)

Table S1. Specific surface area (SSA) and pore volume of PPU, $Pd(OAc)_2$@PPU and Pd@PPU

Sample	PPU	$Pd(OAc)_2$@PPU	Pd@PPU
SSA (m^2/g)	154.98	151.01	143.07
Pore volume (cm^3/g)	0.64	0.62	0.61

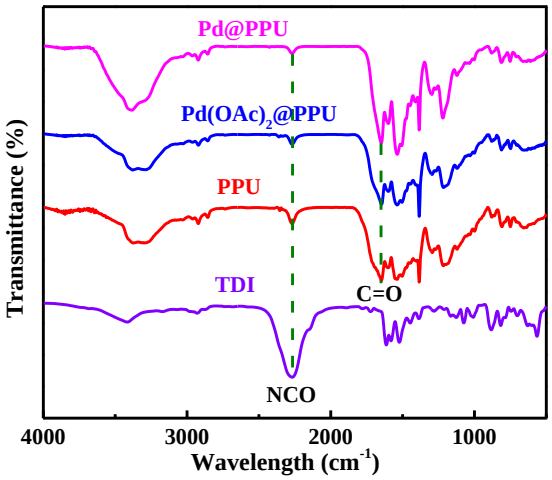

Figure S3. FTIR spectra of TDI, PPU, $Pd(OAc)_2$@PPU and Pd@PPU

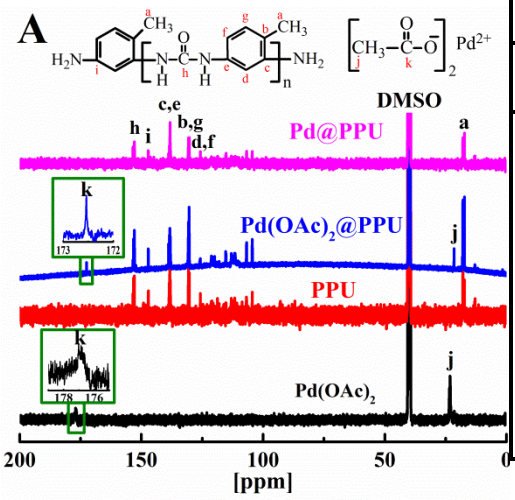

B	Chemical shift δ (ppm)			
C	$Pd(OAc)_2$@PPU	Pd@PPU	PPU	$Pd(OAc)_2$
C_a	17.27	17.27	17.27	-
C_b, C_g	130.36	130.36	130.36	-
C_c, C_e	138.32	138.32	138.32	-
C_d, C_f	125.76	125.76	125.76	-
C_h	152.89	152.89	152.89	-
C_i	147.16	147.16	147.16	-
C_j	21.56	-	-	23.17
C_k	172.54	-	-	177.02

Figure S4. ^{13}C NMR spectra (A) and the chemical shifts (B) of $Pd(OAc)_2$, PPU, $Pd(OAc)_2$@PPU and Pd@PPU

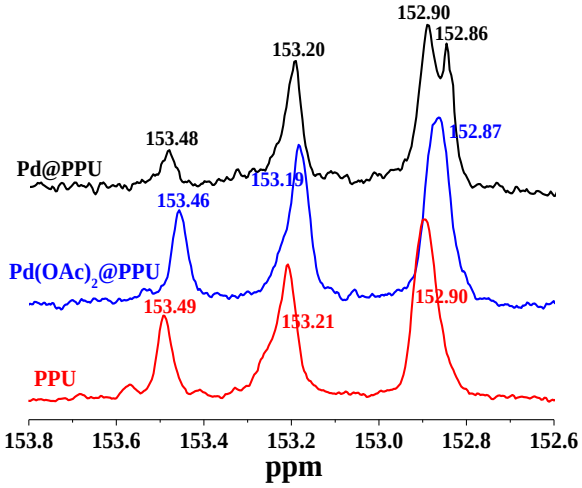

Figure S5. Enlarged ^{13}C NMR spectra (from 153.8 to 152.6 ppm) of PPU, $Pd(OAc)_2$@PPU and Pd@PPU

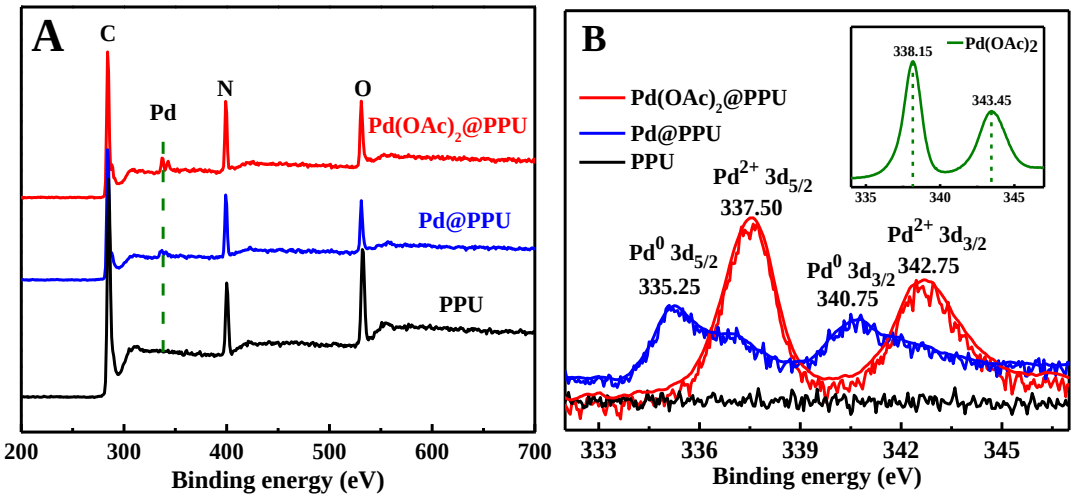

Figure S6. XPS survey spectra of PPU, $Pd(OAc)_2$@PPU and Pd@PPU (A), and their enlarged spectra from 332 to 346 eV around Pd binding region (B) plus that of $Pd(OAc)_2$ (B, inset)

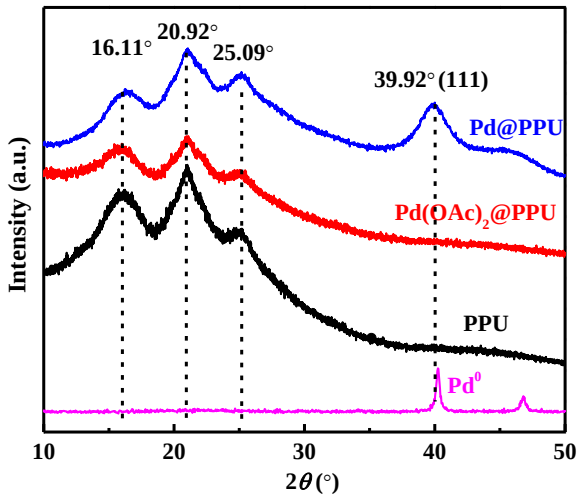

Figure S7. XRD diffractograms of PPU, $Pd(OAc)_2$@PPU, Pd@PPU and that of Pd powder obtained from direct reduction of $Pd(OAc)_2$ by $NaBH_4$

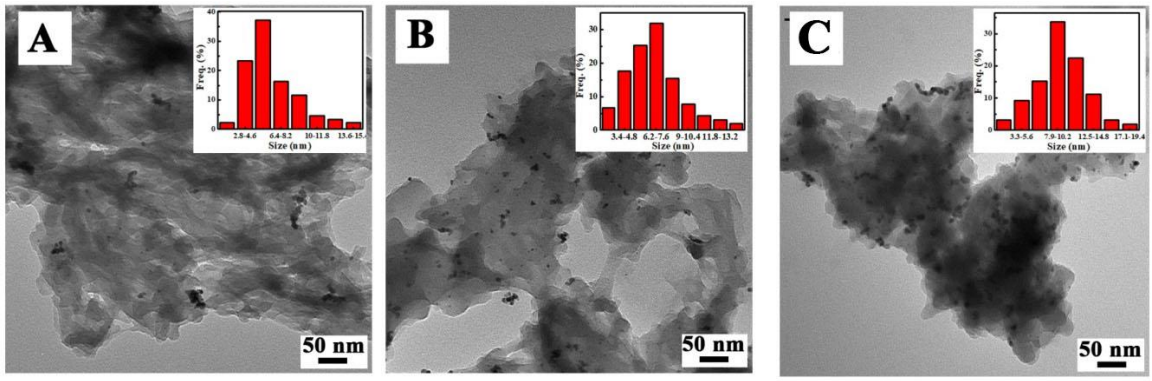

Figure S8. TEM images of Pd@PPU with different Pd content loaded on PPU: 1.91 wt% (A), 2.41 wt% (B), 2.87 wt% (C) and the size distribution of Pd-NPs（insets)

Table S2. Sizes of Pd-NPs in Pd@PPU catalysts of different Pd content

$Pd(OAc)_2$@PPU			Pd@PPU	
PPU-$Pd(OAc)_2$ contact time (h)	Pd(II) (wt%)	Average size (nm)	Pd (wt%)	Average size (nm)
10	1.87	-	1.91	5.67
40	2.35	-	2.41	6.50
50	2.48	1.27	2.55	7.18
80	2.79	-	2.87	9.53

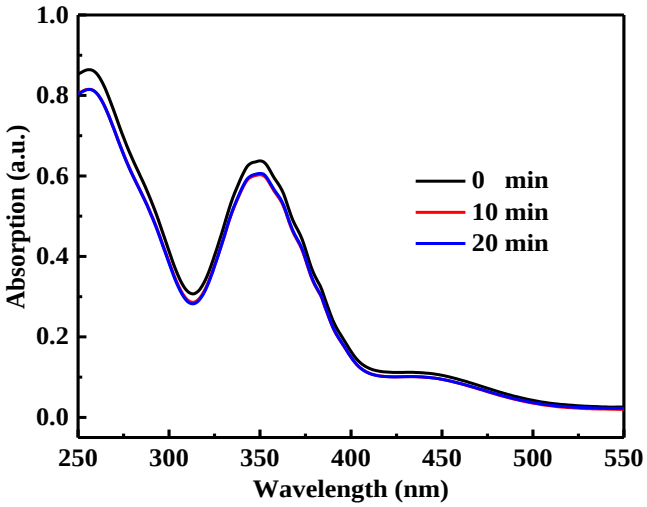

Figure S9. UV-vis absorbance of the supernatant in Cr(VI) reduction with the catalyst Pd@PPU replaced by $Pd(OAc)_2$@PPU (Reaction conditions: $K_2Cr_2O_7$, 2.00 mM; FA, 0.583 M; SF, 0.244 M; $Pd(OAc)_2$@PPU of 2.48 wt% of Pd(II), 0.59 mg/mL)

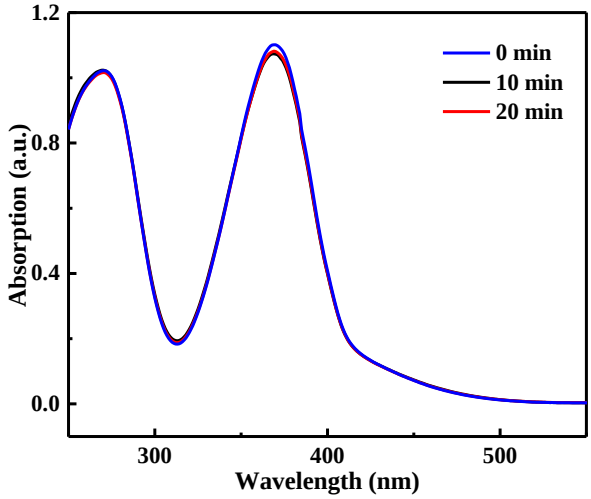

Figure S10. UV-vis spectra of the supernatant in $K_2Cr_2O_7$ (2.00 mM) reduction at 25 °C in the presence of Pd@PPU (of 2.55 wt% of Pd, 0.59 mg/mL) without FA (other conditions were same as in Figure S9)

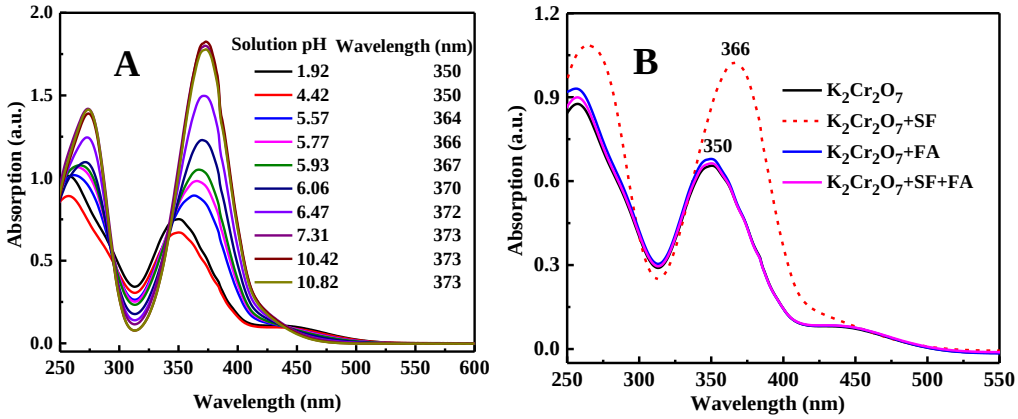

Figure S11. UV-vis spectra of $K_2Cr_2O_7$ aqueous solution (2.00 mM) at different pH (A), and those of solutions of $K_2Cr_2O_7$ (2.00 mM) alone, in the presence of SF (0.244 M), FA (0.583 M), and both SF (0.244 M) and FA (0.583 M) (B)

Table S3. pH of aqueous solution of $K_2Cr_2O_7$ in the presence of different chemicals

Aqueous solution	pH
$K_2Cr_2O_7$ (2.00 mM)	4.42
$K_2Cr_2O_7$ (2.00 mM) and SF (0.244 M)	5.79
$K_2Cr_2O_7$ (2.00 mM) and FA (0.583 M)	1.92
$K_2Cr_2O_7$ (2.00 mM) with SF (0.244 M) and FA (0.583 M)	3.12

Table S4. pH of the reaction mixtures and rate constant (k) in Cr(VI) reduction at different FA concentration

FA (M)	0	0.259	0.389	0.518	0.583	0.648
pH	5.79	3.44	3.32	3.24	3.12	3.02
k (min^{-1})	0.001	0.061	0.117	0.198	0.251	0.252

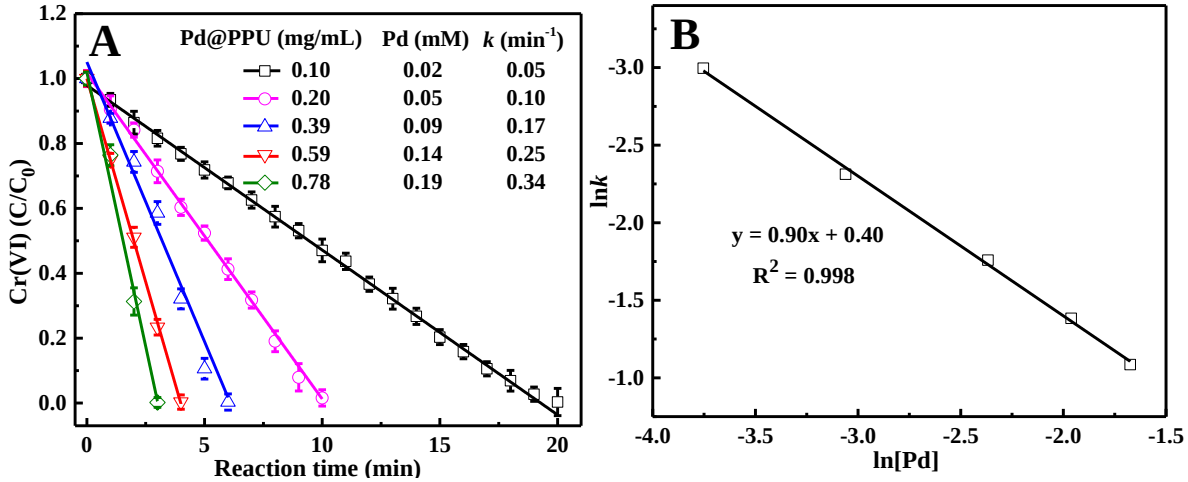

Figure S12. Effect of Pd@PPU (of 2.55 wt% of Pd) amount on Cr(VI) reduction (A), and ln*k* as function of ln[Pd] (B) (Conditions: $K_2Cr_2O_7$, 2.00 mM; FA, 0.583 M; SF, 0.244 M)

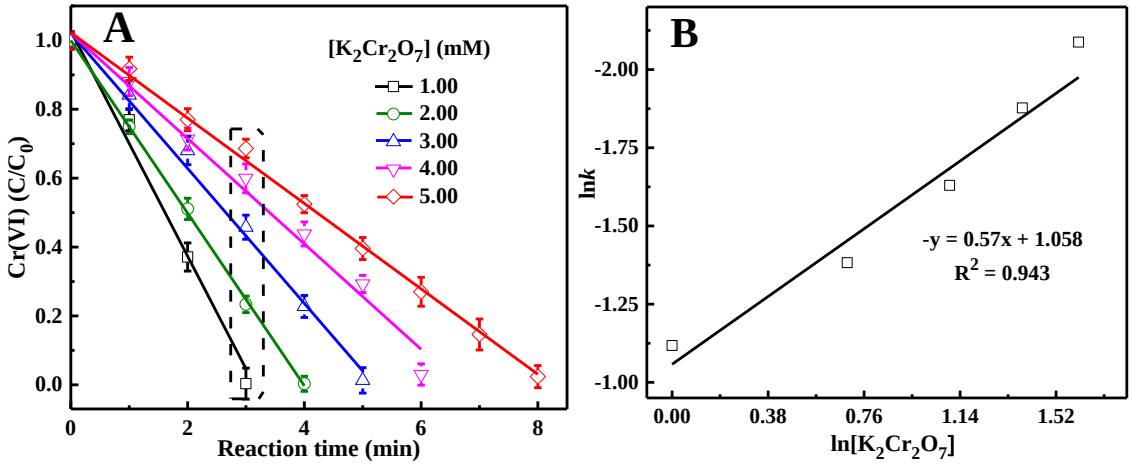

Figure S13. Reduction of Cr(VI) with different initial $K_2Cr_2O_7$ concentrations (A), and their corresponding ln*k* verses ln[$K_2Cr_2O_7$] (B). (Conditions: Pd@PPU of 2.55 wt% of Pd, 0.59 mg/mL; FA, 0.583 M; SF, 0.244 M; 25 °C)

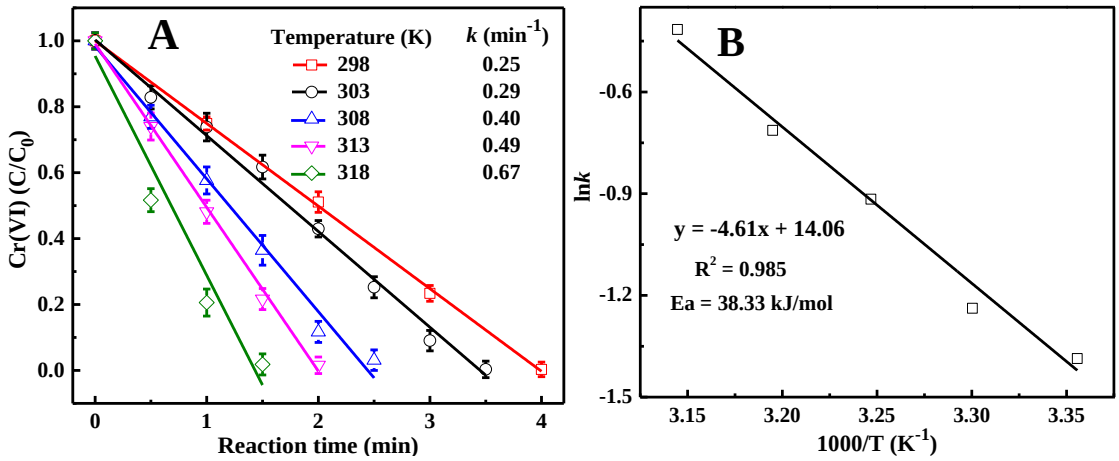

Figure S14. Cr(VI) reduction catalyzed by Pd@PPU at different temperature (A), and logarithm of the rate constant, ln*k*, as function of temperature (1000/T) (B) (Conditions: Pd@PPU of 2.55 wt% of Pd, 0.59 mg/mL; $K_2Cr_2O_7$, 2.00 mM; FA, 0.583 M; SF, 0.244 M)

Table S5. Catalytic properties of some composite catalysts of M-NPs (Pd, Ni, Pt) immobilized on different supports for Cr(VI) reduction with FA as reducer

Catalysts	$[K_2Cr_2O_7]$/NPs (mol.)	t^a (min)	T^b (K)	K (min^{-1})	TOF[c]	Ref.
Pd@SiO_2–NH_2 function	15.15	6	298	0.15	2.53	1
Pd@eggshell membrane	2.51	26	318	0.13	0.10	2
Pd tetrapods	21.05	5	323	0.57	4.21	3
Pd-NPs	12.66	5	318	-	2.53	4
Pd@polymer nanofibers	27.84	12	323	-	2.32	5
Ni@graphene–Cu	0.36	15	298	0.34	0.02	6
Pt@eggshell membrane	4.39	15	318	0.19	0.29	2
Pd@C	14.17	8	298	0.12	1.77	This work
Pd@PPU	14.17	4	298	0.25	3.54	

a). Reduction time; b). Reaction temperature; c). Turn-over-frequency ($mol_{Cr}/mol_{Pd}/min$), which is defined as the ratio of Cr(VI) (mole) to that of Pd (mole) catalyst in a unity of time (min, see Li, M.; Chen, G. *Nanoscale* **2013**, *5*, 11919–11927).

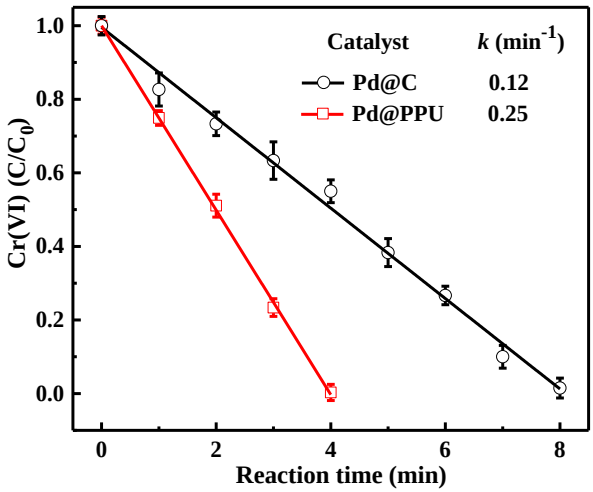

Figure S15. Comparison of catalytic activity of Pd@PPU to commercial Pd@C for Cr(VI) reduction at 25 °C with same Pd amount (Conditions: Pd, 0.015 mg/mL or 0.14 mM; $K_2Cr_2O_7$, 2.00 mM; FA, 0.583 M; SF, 0.244 M)

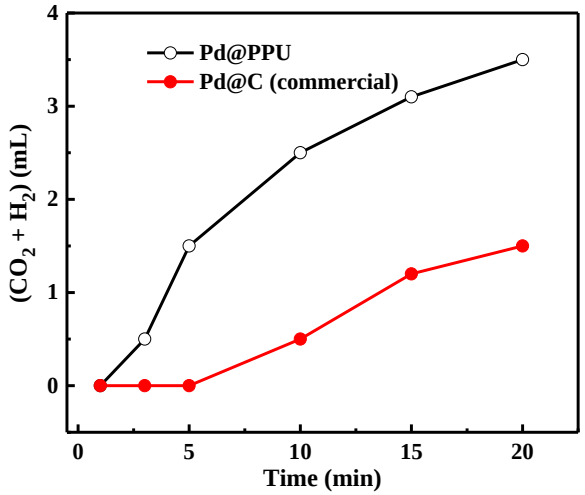

Figure S16. Amounts of gases generated by dehydrogenation of FA in water with Pd@PPU (of 2.55 wt% of Pd, 30.0 mg) and Pd@C (of 10 wt% of Pd, 7.7 mg) at 50 ºC. (FA, 300 µL; SF, 200 mg; H_2O, 10 mL)

Table S6. Dispersion, size and specific surface area (SSA) of Pd-NPs in Pd@PPU and Pd@C obtained from CO pulse chemisorption

Sample	Pd content (wt%)	NPs size* (nm)	SSA (m^2/g)	Dispersion (%)	Pd-NPs' SSA (m^2/g)
Pd@PPU	2.55	4.08 (7.18)	5.13	45.20	201.32
Pd@C	9.96	10.78 (13.25)	4.63	9.20	46.32

(*) size of Pd-NPs from chemisorptions, and the value in parentheses from HRTEM

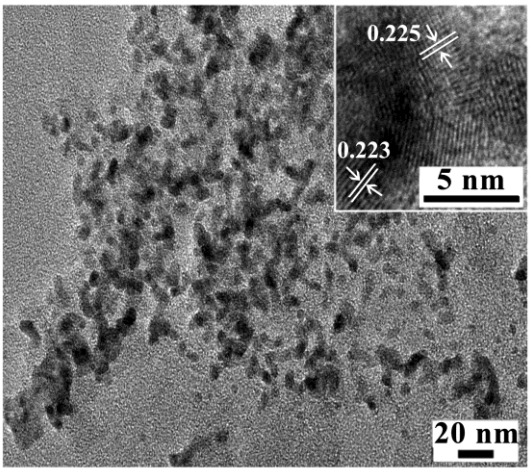

Figure S17. HRTEM picture of Pd@C

Table S7. Reusability of Pd@PPU in Cr(VI) reduction (Pd@PPU, of 2.55 wt% of Pd, 0.59 mg/mL; $K_2Cr_2O_7$, 2.00 mM; FA, 0.583 M; SF, 0.244 M; temperature, 25 °C)

Cycle	Reaction time (min)	Cr(VI) reduction (%)			Average Cr(VI) reduction (%)
1	4	99.67	99.91	99.76	99.78
2	4	99.25	99.35	99.41	99.34
3	4	98.14	97.42	98.81,	98.12
4	4	95.73	96.51	96.61	96.28
5	4	92.75	94.67	92.31	93.24
6	4	89.75	88.67	89.51	89.31

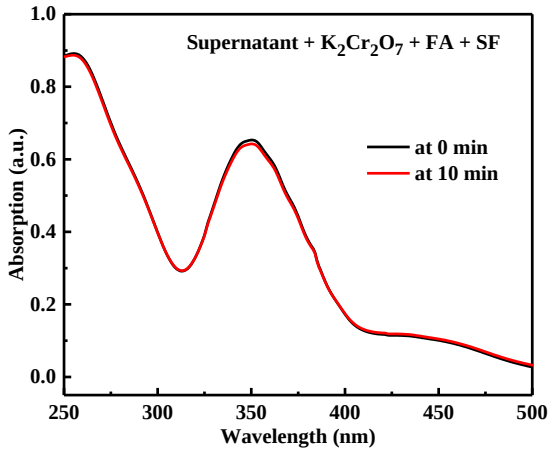

Figure S18. Test of Pd leaching from catalyst by making Cr(VI) solution using the supernatant separated from a previous Cr(VI) reduction instead of water without adding Pd@PPU ($K_2Cr_2O_7$, 2.00 mM; FA, 0.583 M; SF, 0.244 M)

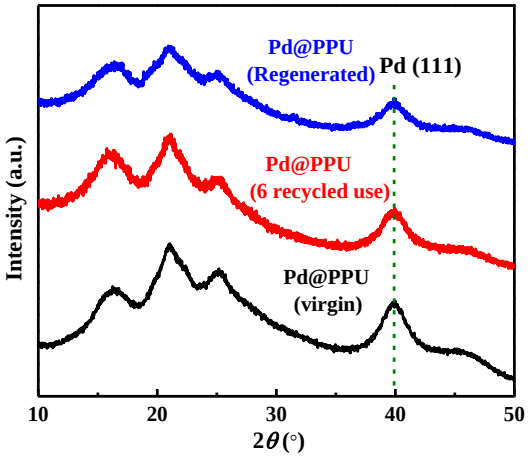

Figure S19. XRD diffractograms of the virgin Pd@PPU (bottom), after 6 recycled uses (middle) and that of the regenerated after 6 recycled uses by heating at 180 °C for 2 h under N_2 atmosphere (upper).

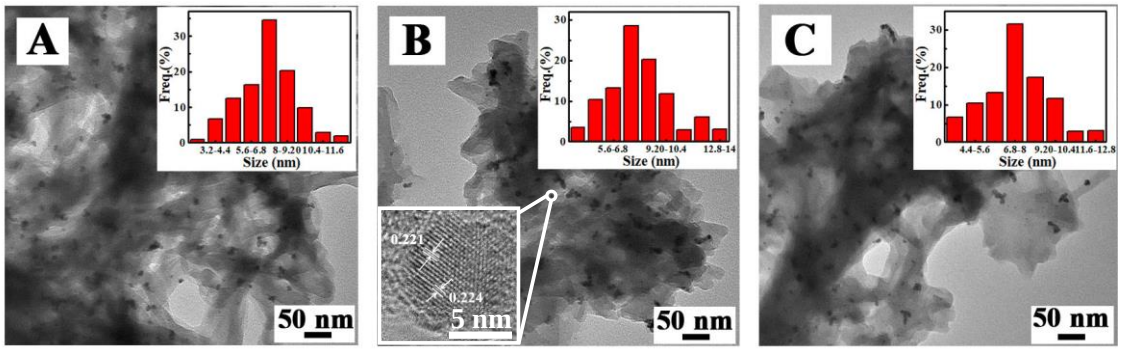

Figure S20. TEM images of virgin Pd@PPU (A, average size of Pd-NPs: 7.18 nm), after 6 recycled uses (B, size of Pd-NPs: 7.92 nm; insert picture in left corner is HRTEM of a Pd-NP), and Pd@PPU regenerated at 180 °C under the flow of N_2 for 2 h (C, size of Pd-NPs: 7.52 nm)

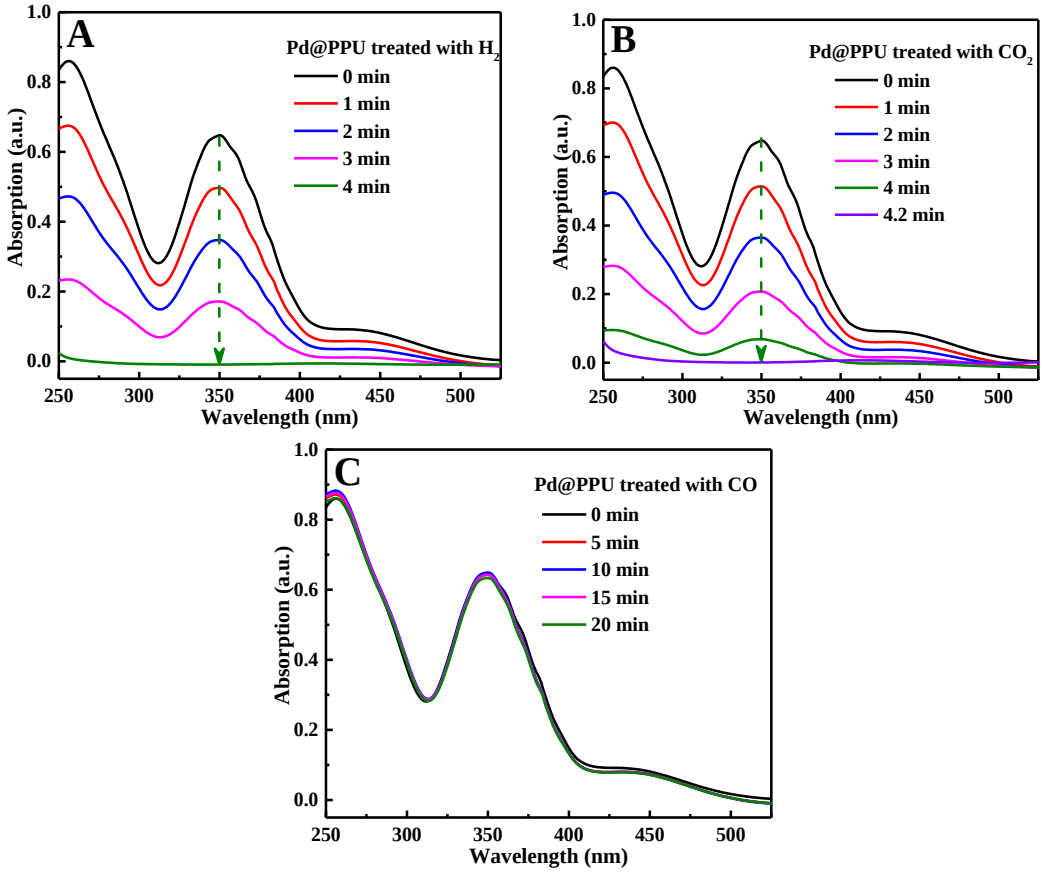

Figure S21. Evolution of UV-vis spectra in Cr(VI) reduction in aqueous phase at 25 °C with pretreated Pd@PPU as the catalyst: pretreated with H_2 (A), CO_2 (B) and CO (C) (Reaction conditions: $K_2Cr_2O_7$, 2.00 mM; FA, 0.583 M; SF, 0.244 M; Pd@PPU of 2.55 wt% of Pd, 0.59 mg/mL)

Table S8. Catalytic activity of Pd@PPU regenerated after 6 recycled uses followed by regeneration by heating it at 180 °C for different time and the color change of PPU when heating at 180 °C for different time (Pd@PPU of 2.55 wt% of Pd, 0.59 mg/mL; $K_2Cr_2O_7$, 2.00 mM; FA, 0.583 M; SF, 0.244 M).

Pd@PPU heating time (h)	Cycle	Reaction time (min)	Cr(VI) reductions (%)		Average reductions (%)	PPU color
1	1	4	95.15	93.42	94.29	No change
2	1	4	99.51	99.43	99.47	No change
3	1	4	77.33	75.46	76.39	Yellowing

References cited in Supporting Information:

(1) Celebi, M.; Yurderi, M.; Bulut, A.; Kaya, M.; Zahmakiran, M. Palladium Nanoparticles Supported on Amine-Functionalized SiO_2 for the Catalytic Hexavalent Chromium Reduction. *Appl. Catal. B: Environ.* **2016**, *180*, 53–64.

(2) Liang, M.; Su, R.; Qi, W.; Zhang, Y.; Huang, R.; Yu, Y.; Wang, L.; He, Z. Reduction of Hexavalent Chromium Using Recyclable Pt/Pd Nanoparticles Immobilized on Procyanidin-Grafted Eggshell Membrane. *Ind. Eng. Chem. Res.* **2014**, *53*, 13635−13643.

(3) Fu, G.; Jiang, X.; Wu, R.; Wei, S.; Sun, D.; Tang, Y.; Lu, T.; Chen, Y. Arginine-Assisted Synthesis and Catalytic Properties of Single-Crystalline Palladium Tetrapods. *ACS Appl. Mater. Interfaces* **2014**, *6*, 22790–22795.

(4) Omole, M. A.; K'Owino, I. O.; Sadik, O. A. Palladium Nanoparticles for Catalytic Reduction of Cr(VI) Using Formic Acid. *Appl. Catal. B: Environ.* **2007**, *76*, 158–167.

(5) Huang, Y.; Ma, H.; Wang, S.; Shen, M.; Guo, R.; Cao, X.; Zhu, M.; Shi, X. Efficient Catalytic Reduction of Hexavalent Chromium Using Palladium Nanoparticle-Immobilized Electrospun Polymer Nanofibers. *ACS Appl. Mater. Interfaces* **2012**, *4*, 3054–3061.

(6) Liu, L.; Xue, J.; Shan, X.; He, G.; Wang, X.; Chen, H. In-Situ Preparation of Three-Dimensional Ni@Graphene-Cu Composites for Ultrafast Reduction of Cr(VI) at Room Temperature. *Catal. Commun.* **2016**, *75*, 13–17.